Cretaceous Research 55 (2015) 116–128

Contents lists available at ScienceDirect

Cretaceous Research

journal homepage: www.elsevier.com/locate/CretRes

U–Pb zircon ages from the northern Austral basin and their correlation with the Early Cretaceous exhumation and volcanism of Patagonia

Matías C. Ghiglione [a,*], Maximiliano Naipauer [a], Christian Sue [b], Vanesa Barberón [a], Victor Valencia [c], Beatriz Aguirre-Urreta [a], Victor A. Ramos [a]

[a] Instituto de Estudios Andinos – CONICET, Universidad de Buenos Aires, Argentina
[b] Franche-Comté University, CNRS-UMR6249, France
[c] School of Earth and Environmental Sciences, Washington State University, USA

ARTICLE INFO

Article history:
Received 27 October 2014
Accepted in revised form 15 February 2015
Available online

Keywords:
Patagonia
Early Cretaceous
Patagonian Andes
Austral basin
Magallanes basin
Opening of the Atlantic Ocean
U–Pb geochronology
Detrital zircons

ABSTRACT

The end of the Early Cretaceous sag stage along the Southern Patagonian Andes is indicated by the sudden appearance of shallow marine to deltaic sandstones on top of deep marine facies. We studied the detrital and volcanic zircon U–Pb geochronology from the coarse-grained deposits represented by the Río Belgrano and Río Tarde formations at the northern end of the Austral or Magallanes basin. The maximum depositional age of the basal green sandstones of Río Belgrano Formation is marked by a ~122 Ma age peak. The youngest single zircon of the overlaying lower Río Tarde Formation yields an age of 118 ± 2 Ma, however the ~122 Ma age peak is equally present. The upper Río Tarde Formation yielded a 112 ± 2 Ma U–Pb zircon age for a volcanic tuff. The ~122 Ma significant peak and 112 ± 2 Ma tuff represent volcanic ash fall coeval with plutonic activity dated between 125 and 110 Ma in the North Patagonian Batholith. An abundant detrital Mesozoic population is present in both units, including a 189-170 Ma peak corresponding to the V1 Jurassic volcanic stage cropping out in the North Patagonian Massif. However, zircons of 153–157 Ma representing the age of Jurassic volcanism along the Patagonian basement domain to the west are scarce. Our data indicate a ~122 Ma age for the studied samples, during which the Southern Patagonian Andes received mixed basement and V1 Jurassic volcanic stage detritus. These combined sources are an outstanding characteristic of the North Patagonian and Deseado massifs, in agreement with the previously proposed Aptian uplift and exhumation of Patagonia.

1. Introduction

The Aptian-Cenomanian evolution of the Southern Patagonian Andes and extra-Andean Patagonia can be represented by two opposing tectonic scenarios: opening of the Atlantic Ocean to the east and subduction processes along the pacific margin of South America to the west (Fig. 1). Before that period, a major change in the Southern Atlantic Ocean occurred, from Valanginian-Hauterivian pre-breakup extension, to latest Barremian-Albian post-breakup deformation (Torsvik et al., 2007; Dalziel et al., 2013; Heine et al., 2013). Uplift and exhumation during post-breakup deformation is suggested by an angular unconformity separating subhorizontal late Aptian sequences from underlying faults and folds in the San Julián offshore basin (Fig. 1; Figueiredo et al., 1996; Homovc and Constantini, 2001). The Aptian angular unconformity, identified in seismic lines, can be correlated with a paraconformity at the base of the Baqueró Group outcropping in the Deseado Massif (Fig. 1; Soares et al., 2000). The pyroclastic Baqueró Group, dated between ~118 and 114 Ma (Corbella, 2001; Césari et al., 2011; Pérez Loinaze et al., 2013) is regarded as equivalent to volcanic Divisadero Formation of the Northern Patagonian Andes (Corbella, 2006). The Divisadero Formation is constrained between 118 and 116 Ma (Pankhurst et al., 2003), and was deposited on top of an angular unconformity indicating an early Aptian compressional event (De La Cruz et al., 2003). There are also suggestions that some structures along the North Patagonian Massif suffered compression during the same time-span (Suárez et al., 2010). Nevertheless, the effects of Early Cretaceous

* Corresponding author.
E-mail address: matias@gl.fcen.uba.ar (M.C. Ghiglione).

http://dx.doi.org/10.1016/j.cretres.2015.02.006
0195-6671/

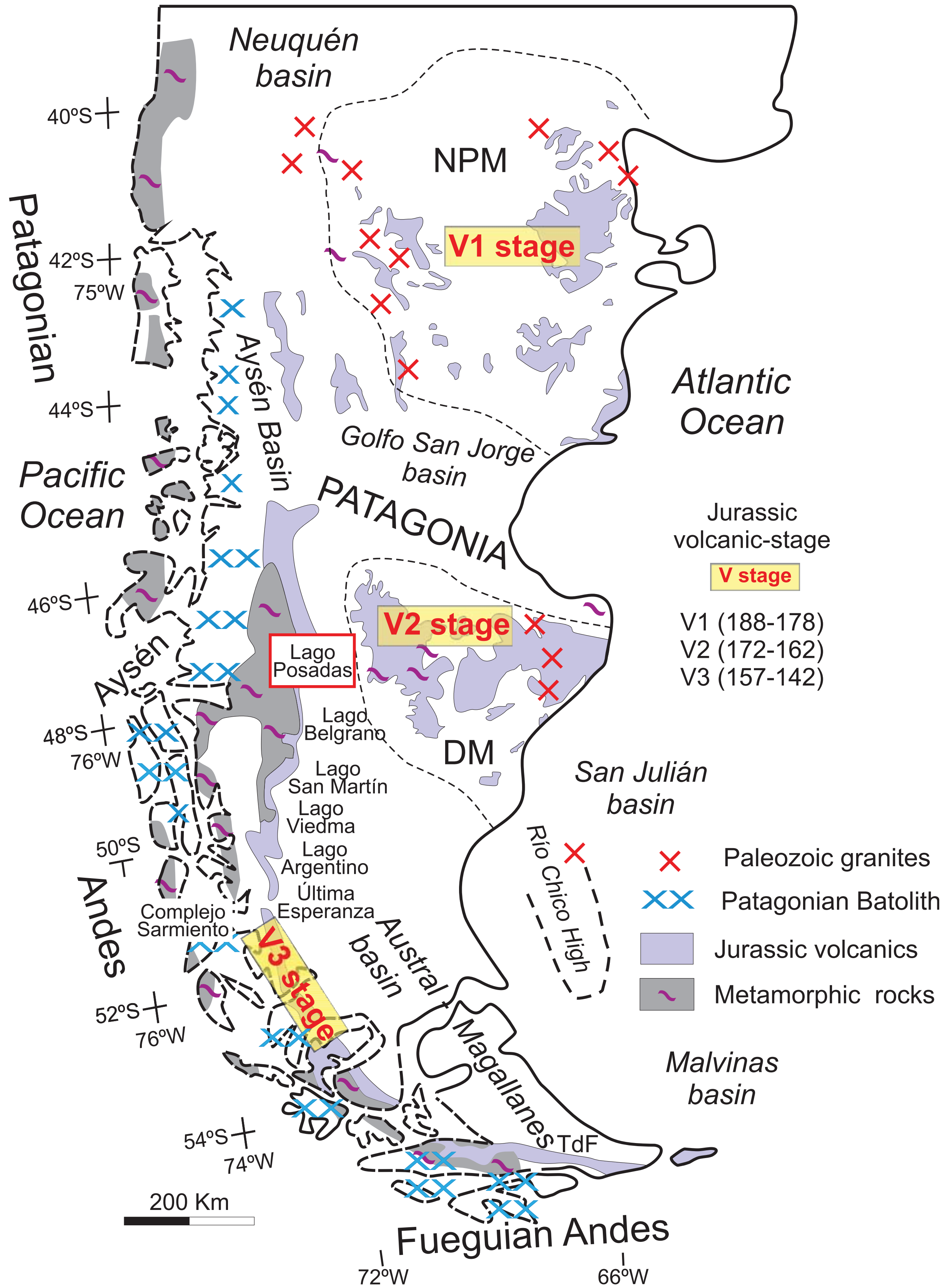

Fig. 1. Location of the study zone and localities mentioned in the text. Red square shows location of geological map of Fig. 3. Basement and igneous detrital sources from Patagonia are shown; see text for discussion. Jurassic volcanic-stages from Pankhurst et al. (2000). DM: Deseado Massif; NPM: North Patagonian Massif; TdF: Tierra del Fuego Island.

exhumation and erosion of central Patagonia and the Northern Patagonian Andes implied by the Aptian unconformity have not been assessed yet in the overall framework of the Austral or Magallanes basin.

These events were followed by Late Cretaceous uplift along the orogenic edge of the Southern Patagonian Andes (Fig. 1). The ensuing foreland stage in the Austral basin is indicated by the appearance of coarse sandstones on top of the sag deposits (Wilson, 1991). Foreland deposits in the Última Esperanza region (Katz, 1963; Wilson, 1991) contain zircon grains derived from Andean sources (Fig. 1), including Paleozoic–Mesozoic metamorphic and ophiolitic complexes, and Upper Jurassic volcanic units (Fildani and Hessler, 2005; Romans et al., 2011). U–Pb data indicate a diachronous sag-to-foreland stratigraphic transition (Fig. 2): from before 96 Ma in Lago San Martín (Mata Amarilla Formation; Varela et al., 2012) and ~101 Ma in Última Esperanza (Punta Barrosa Formation; Fosdick et al., 2011) to ~85–89 Ma in Tierra del Fuego (McAtamney et al., 2011). Therefore an important question remaining was whether this trend continues to the established northern end of the basin in Lago Pueyrredón-Posadas (Fig. 2).

We studied the northern outcrops of the Austral basin Cretaceous depocenter at 47°30′S, on the southwestern shore of Lago Pueyrredón-Posadas (Fig. 3). The site is located in the foothills of the Southern Patagonian Andes, and west of the Patagonian basement massifs (Fig. 1). In this region, Lower Cretaceous deltaic regressive sequences of the Río Belgrano and Río Tarde formations are covering the sag (Fig 2; Aguirre-Urreta, 1990). We applied U–Pb geochronology in detrital and volcanic zircons from the regressive sequences, revealing a ~122 Ma maximum age for the post-sag stage. Comparison of the obtained U–Pb age spectra for detrital zircon population, together with stratigraphic and tectonic considerations suggest that the Early Cretaceous sedimentary and volcanic evolution of the northern Austral basin was related to geodynamic processes of extra-Andean Patagonia.

2. Regional geologic framework: source zones and sedimentary basins

There are some strong common elements in the Mesozoic tectonic history of South America south of 41°S, comprising Patagonia and the Patagonian-Fueguian Andes (Fig. 1). Initial extensional subsidence began during the Triassic-Jurassic continental rifting of Gondwana, characterized by rhyolitic ignimbrites with minor mafic lavas (Uliana et al., 1989). Magmatism associated with these extensional depocenters is clearly diachronous, following a southwestward migration path. Volcanism spanned more than 40 myrs during three stages defined by peak activity (Fig. 1; Pankhurst et al., 2000): V1 (188–178 Ma) in the North Patagonian Massif, V2 (172–162 Ma) in the Deseado Massif and V3 along the Southern Patagonian Andes, spanning 157–153 Ma in the Austral basin (Féraud et al., 1999), to 152–142 Ma in the relict Rocas Verdes basin at Complejo Sarmiento (Calderón et al., 2007). The synrift sequences (El Quemado Complex, Tobífera Formation) are overlain by extended Lower Cretaceous sag deposits of the arenaceous Springhill, and pelitic Zapata-Río Mayer formations (Fig. 2).

Initial compression in the Southern Patagonian Andes involved closure of the Rocas Verdes basin during the Late Cretaceous, and obduction of its oceanic crust from 85 Ma (Calderón et al., 2012). South of 50°S, the Upper Cretaceous-Cenozoic Austral and Malvinas foreland basins developed a widespread continuous marine depocenter more than 1000 km long and 500 km wide, with subsidence concentrated along the cordilleran front (Fig. 1; Biddle et al., 1986; Ghiglione et al., 2009, 2010; Baristeas et al., 2013). Sediments came mainly from the rising hinterland, with a dominant north to south sediment dispersal pattern (Wilson, 1991).

2.1. Austral basin

In the present work, we recognize two segments, north and south of 49–50°S at Lago San Martín, with different and distinctive post-sag Cretaceous sequences (Fig. 2; Ghiglione et al., in press). The northernmost sector at Lago Posadas (47°S; Fig. 1) presents prograding deltaic and fluvial deposits of the Río Belgrano and Río Tarde formations, topped by up to 250 m of tuffs and volcaniclastic deposits (Fig. 2). The Río Belgrano Formation has Hauterivian-Barremian ammonites, with outcrops restricted to the area between Lago Posadas and Lago San Martín (Aguirre-Urreta, 1990, 2002). The Aptian-Cenomanian Río Tarde Formation represents the first coarse-grained fluvial deposits (Arbe, 1986; Ramos, 1989).

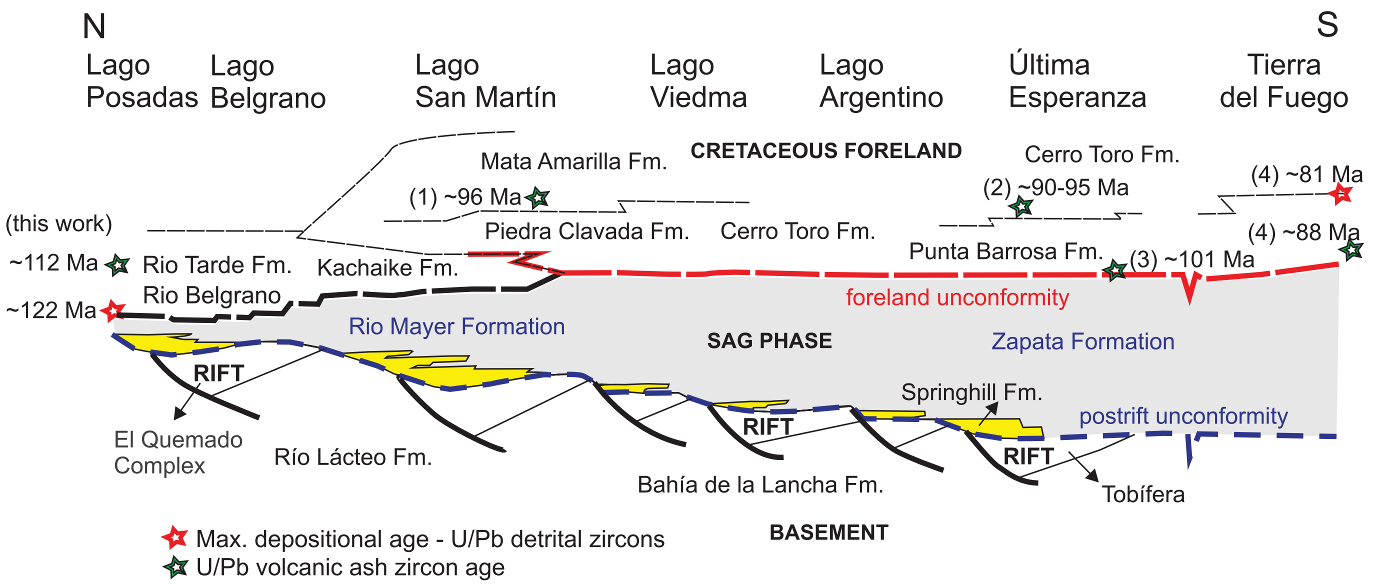

Fig. 2. North–South oriented schematic stratigraphic cross-section modified from the "Río Mayer and Lago San Martin Cycles" of Arbe (2002) showing lateral correlation of lithotectonic sequences and formations described in the text. Bracketed numbers indicates references: (1) Varela et al. (2012); (2) Bernhardt et al. (2012); (3) Fosdick et al. (2011); (4) McAtamney et al. (2011). See localities in Fig. 1.

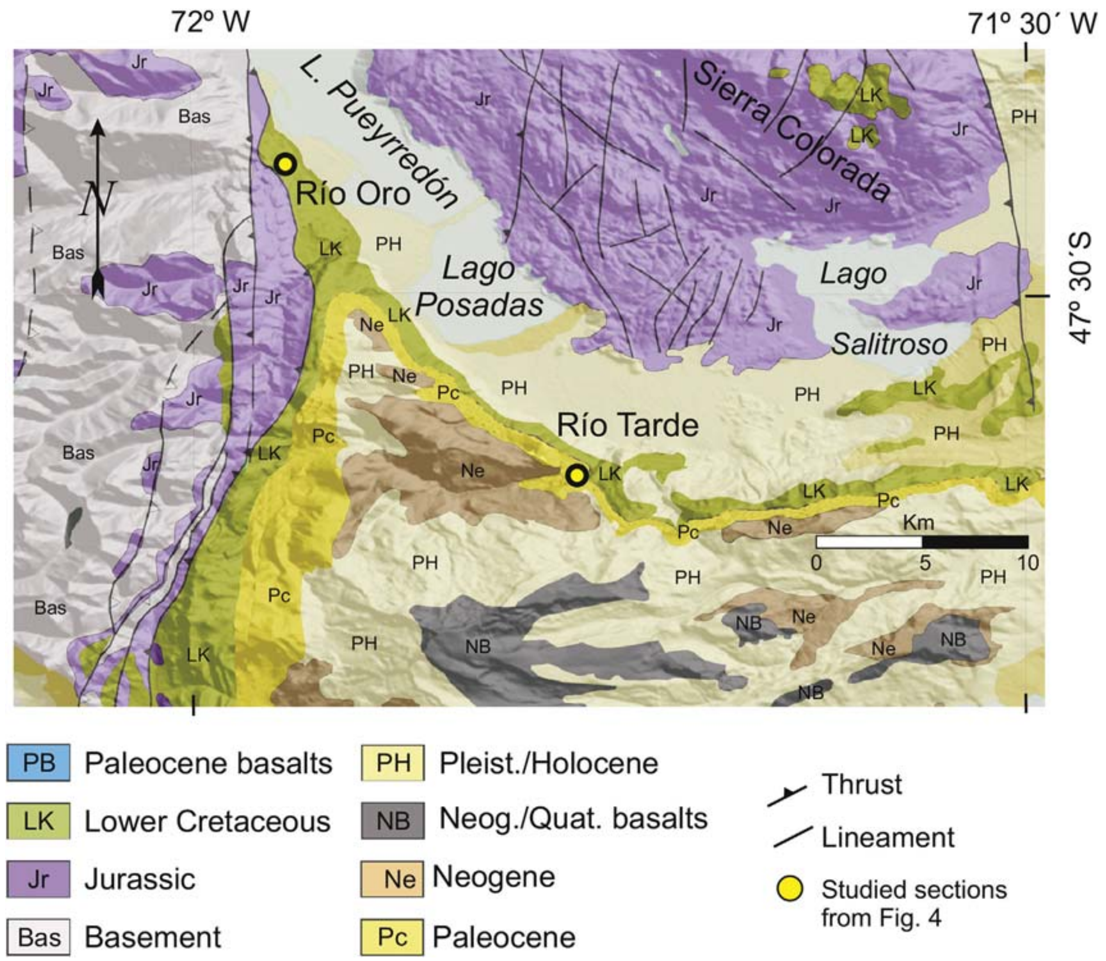

Fig. 3. Geological sketch of the study zone. Modified from Giacosa and Franchi (2001). See location in Fig. 1.

First marine regressive units south of Lago Viedma (Figs. 1 and 2) are represented by the lower Cerro Toro Formation in Argentina (Kraemer and Riccardi, 1997) regarded as equivalent to Punta Barrosa Formation of Chile (Ghiglione et al., 2014). Sandstone petrography, detrital zircon geochronology, and mudstone geochemistry indicate that the Cenomanian-Turonian Punta Barrosa Formation and equivalent units in Tierra del Fuego were derived from the west (Fildani and Hessler, 2005; McAtamney et al., 2011). Fosdick et al. (2011) dated a volcanic ash at the Zapata/Punta Barrosa formations transition zone yielding a U–Pb zircon age of 101 ± 1 Ma (Fig. 2) showing that incipient thrust belt formation was under way as early as the latest Albian. The following Coniacian-Danian sequences have detrital zircons with abundant Tobífera volcanic zircons (V3 volcanic stage; 157–145 Ma), Cretaceous arc material (110–70 Ma), and minor components of Paleozoic basement (Romans et al., 2011).

2.2. Extra-Andean Patagonia

East and northeast of our study zone Paleozoic metasedimentary and plutonic units of extra-Andean Patagonia crop out in the Deseado and North Patagonian massifs (Fig. 1). The reader is referred to Ramos and Naipauer (2014) for a detailed account of those outcrops.

The igneous and metamorphic rocks are covered in angular unconformity by a Jurassic volcanism composed by rhyolitic ignimbrites and andesite and basaltic andesite lavas. This volcanics are grouped in the Chon Aike magmatic province, which corresponds to volcanic stages V1 and V2 from Pankhurst et al. (2000). In the V1 are grouped rhyolites of the Marifil Formation and andesite and basaltic andesites of Taquetrén and Lonco Trapial formations exposed in the North Patagonian Massif (Fig. 1). The V1 ages between 188 and 178 Ma were obtained from Rb–Sr, Ar–Ar, and U–Pb (Pankhurst and Rapela, 1995; Féraud et al., 1999; Bertrand et al., 1999; Pankhurst et al., 2000; Cúneo et al., 2013). The V2 stage comprises ignimbrites of the Chon Aike Formation and volcaniclastic strata of the La Matilde Formation, both units exposed in the Deseado Massif (Fig. 1). U–Pb and Rb–Sr ages indicate a V2 magmatic activity peak at 172–162 Ma (Pankhurst et al., 2000).

The Deseado and San Julian basins evolved during the Mesozoic as continental intracratonic rifts developed above the metamorphic and volcanic basement, in response to regional pre-breakup extension (Homovc and Constantini, 2001). Seismic sections show a prominent Aptian angular unconformity that can be followed regionally, marking late Valanginian–Aptian wrenching that produced transpressive structures in both basins (Figueiredo et al., 1996; Giacosa et al., 2010). The angular unconformity can be correlated with the paraconformity separating the Baqueró Group from the Bajo Grande Group in the Deseado Massif (Soares et al., 2000; Homovc and Constantini, 2001). The Baqueró Group is divided from bottom to top in Anfiteatro del Ticó, Bajo del Tigre and Punta del Barco formations. The Punta del Barco Formation has been recently dated at 114.7 ± 0.2 Ma (Césari et al., 2011), and a basal tuff in the Anfiteatro del Ticó Formation yielded a CA-TIMS U–Pb zircon age of 118.2 ± 0.1 Ma (Pérez Loinaze et al., 2013). These results are in agreement with previous ~118 Ma $^{40}Ar/^{39}Ar$

ages from the Anfiteatro de Ticó Formation (Corbella, 2001). These ages constrain the proposed deformation of the Deseado and San Julian basins as occurring before 118 Ma.

2.3. Patagonian Andes

The older basement (Fig. 2) is composed of Devonian to Carboniferous metasedimentary (Río Lácteo Formation) and sedimentary (Bahía La Lancha Formation) rocks with high ductile deformation (Ramos, 1989; Giacosa and Márquez, 2002). These two units are part of the Eastern Andean Metamorphic Complex (Hervé et al., 2008) developed to the west and north of the study area, mainly in Chile (Fig. 1). Detrital zircon ages (U–Pb SHRIMP) for the Bahía La Lancha Formation obtained by Augustsson et al. (2006), have a maximum at ~345 and other peaks at 383, 509 and 625 Ma, with subordinate early Neoproterozoic and Mesoproterozoic ages. Along the eastern margin of the Southern Patagonia Andes, the metamorphic basement is cover by Late Jurassic volcanic rocks (Fig. 2) of the El Quemado Complex (Argentina) and Ibañez and Tobífera formations (Chile). This volcanism is included in the V3 volcanic stage with ages between 157 and 145 Ma (Féraud et al., 1999; Pankhurst et al., 2000, 2003; Calderón et al., 2007). Along the northeastern outcrops of the study region, in the Sierra Colorada (Fig. 3), ignimbrites of El Quemado Formation were dated by U–Pb zircons at 154 ± 2 Ma (Pankhurst et al., 2000) and $^{40}Ar/^{39}Ar$ at 156 ± 2 Ma (Iglesia Llanos et al., 2003).

The Paleozoic basement and the Jurassic volcanic rocks are the host rocks of the Meso-Cenozoic Patagonian Batholith (Fig. 1; Hervé et al., 2007, 2008; Ramos and Ghiglione, 2008). Southwest of the study area the batholith is represented by the Miocene granitic San Lorenzo pluton that yielded 6.5 ± 0.5 Ma, K/Ar biotite ages (Welkner et al., 2002).

To the west, in the Aysén region of Chile (Fig. 1), several Upper Jurassic - Cretaceous granitoids were dated by U–Pb and $^{40}Ar/^{39}Ar$ between 150 and 69 Ma (Pankhurst et al., 1999; Suárez and De la Cruz, 2001; Thomson et al., 2001) including a cluster of ages between 125 and 110 Ma. In this region, an angular unconformity separates the Divisadero Group from the folded underlying Lower Cretaceous volcanic and sedimentary rocks of the Coyhaique Group (Suárez and De la Cruz, 2001). The Divisadero Group in Chile was dated by K–Ar and Ar–Ar, with ages ranging from ~118 to 113 Ma (De La Cruz et al., 2003; Suárez et al., 2010), and four U–Pb SHRIMP zircon ages yielding between ~118 and 116 Ma (Pankhurst et al., 2003). These ages, together with structural considerations, indicate that the Río Mayo Embayment or Aysén basin (Fig. 1) was inverted between 121 and 118 Ma (Suárez et al., 2010).

3. Stratigraphy

The Río Mayer Formation is dominated by black shales interspersed with fine sandstones of restricted platform facies. The contacts are transitional with both the sandstones and conglomerates of the underlying Springhill Formation, and with the overlying Río Belgrano Formation (Fig. 4). Aguirre-Urreta and Ramos (1981) estimate the beginning of the sedimentation for this unit as Valanginian-Hauterivian for the northernmost outcrops.

The Río Belgrano Formation in the Río Tarde section (Figs. 3 and 4) is 133 m thick (Homovc, 1980), and at least 160 m at Cuesta del Oro (nortwest from Río Oro; Aguirre-Urreta, 2002). The Río Belgrano Formation has green and gray sandstones intercalated with shales and limestones. It represents a proximal environment near the coastline, with beach and wave channels (Arbe, 1986). A Barremian-Aptian age is based on fossils, especially ammonites (Aguirre-Urreta, 1990, 2002).

The Río Tarde Formation overlies the Río Belgrano Formation in concordance or erosive discordance. The formation is divided into two members based on its pyroclastic content. The lower member is characterized by red conglomerates and sandstones; the contact is transitional with the upper member, dominated by tuffs and tuffaceous sandstones (Fig. 4). Its depositional environment is interpreted as a fluvial system of high energy (Arbe, 1986). The upper member corresponds to floodplains with ash falls, yielding K–Ar ages (biotite and plagioclase) of 97 ± 4 and 99 ± 6 Ma (Ramos and Drake, 1987).

These units are slightly unconformably covered by the Eocene Posadas Basalt, followed by the Oligocene marine Centinela Formation, the Miocene synorogenic deposits of the Santa Cruz Formation, and the Mio-Pliocene Strobel Basalts (Fig. 5A; Ramos, 1989; Giacosa and Franchi, 2001).

3.1. Río Oro section

The sedimentary profile on the SE side of Río Oro (Fig. 3) includes the Río Belgrano and lower Río Tarde formations (Figs. 4 and 5B). Basal thick sandstones of the Río Belgrano Formation lie in concordance over black, ammonite bearing mudstones and limestones in the transition with the Río Mayer Formation (Fig. 5C).

The measured section of the Río Belgrano Formation is composed of 40 m of green, fine to medium sandstones and interspersed fine conglomerates (Fig. 4): The first 9 m includes medium to fine sandstones, with flaser, wavy and cross-bedding, and intercalated conglomeratic sandstones with erosive bottoms. A continuous 2 m thick bed of conglomeratic sandstone follows, containing pelecypods, gastropods and corals. The section continues with 8 m of thinning-upwards medium sandstones in banks 0.5 m thick whose grain size decreases to shale, followed by 6 m of shale and 5 m of fine massive sandstones. The section ends with 10 m of conglomeratic to sandstone thinning-upwards banks with erosive base and parallel to cross-bedding.

The Río Tarde Formation overlies in concordance (Fig. 5B). The measured thickness includes the basal 45 m of the lower member (Fig. 4): the first 12 m are thinning-upwards banks of red conglomerates to medium sandstones, with erosive base, parallel and cross-bedding. The section continues with 11 m of coarse to medium sandstones and tuffs, and 9 m of thinning-upwards red conglomeratic banks, with erosive base. The measured section ends with 7 m of sandstones with silicified trunks. The sedimentary succession continues sporadically up to the coast of Lago Pueyrredón (Fig. 3), but was not measured.

3.2. Río Tarde section

The Río Belgrano Formation is characterized by a 133 m thick succession of fine to medium green sandstones (Fig. 4). Sampling was focalized in the Río Tarde Formation following the section from Homovc (1980): the section starts with 18 m of red conglomerates to coarse sandstones, with cross-bedding and silicified trunks, followed by 25 m of medium sandstones with parallel bedding and silicified trunks. The coarse deposits are covered by 50 m of medium to fine sandstones with parallel, cross-bedding and massive structures. The upper Río Tarde Formation starts with interspersed green tuffs and fine sandstones. Towards the top there are gray sandy tuffs and tuffaceous sandstones, topped by litharenite sandstones with parallel and cross-bedding.

4. Methodology

4.1. Sample selection and petrography

Petrography studies were performed on 15 sandstone, conglomeratic sandstone and volcanic rocks to select samples for U–Pb dating. The samples were studied under a polarized

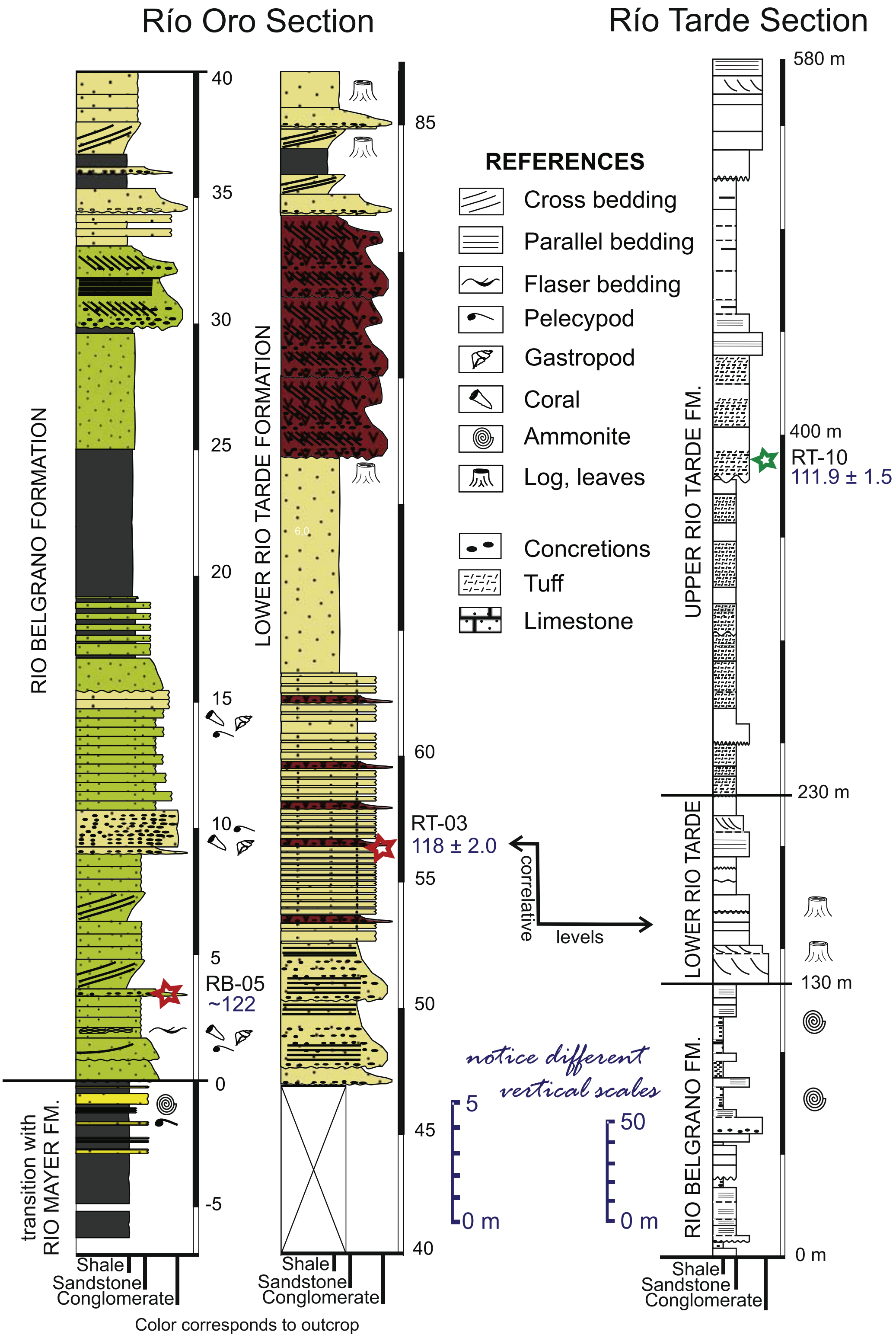

Fig. 4. Stratigraphic column of the Río Belgrano and Río Tarde formations at Río Oro (left) and Río Tarde (right) localities. Notice different scales, left column is 10× with respect to right column. Collected samples and geochronological results are indicated. Río Tarde section is modified after Homovc (1980).

microscope and the sandstones were classified by Barberón et al. (2014), following the scheme of Folk et al. (1970). In the Río Oro section two samples (RB-05 and RT-03) were selected, while in the Río Tarde section only one (RT-10) was picked for U–Pb geochronology (Fig. 4).

Sample RB-05 is a fine feldspathic litharenite with angular to subangular grains. Framework sand grains include monocrystalline quartz, K-feldspar, polycrystalline quartz and lithic fragments of sedimentary, volcanic and low-grade metamorphic rocks. Glauconite, muscovite and zircon are present as accessory minerals. The

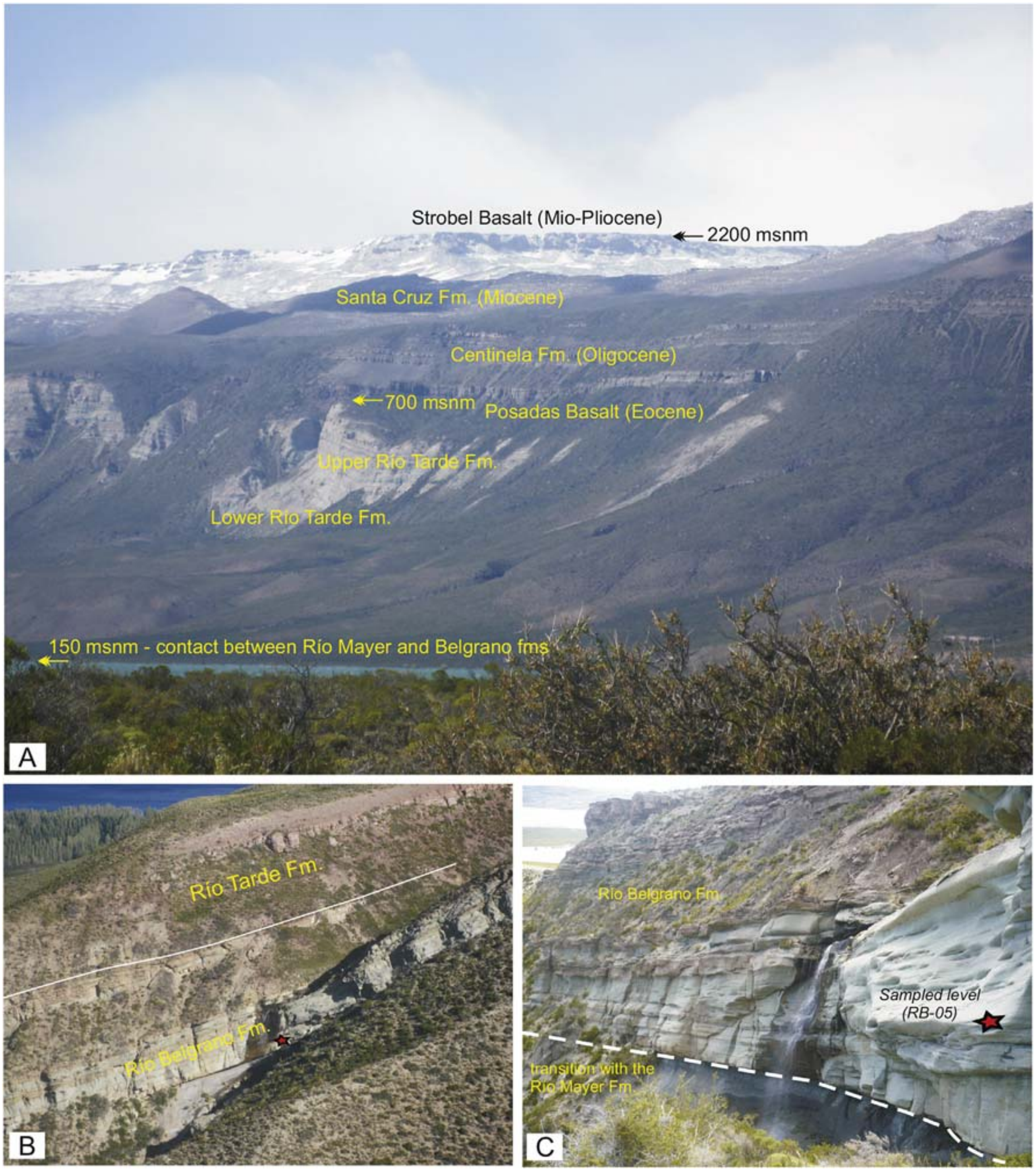

Fig. 5. (A) Stratigraphic panoramic at southwest coast of Lago Posada; view to the SW. The sequence is subhorizontal and altitude measurements are a good approach to real stratigraphic thickness. (B and C) Río Oro section; view to the SE. Contact between black fossil bearing mudstones and limestones from Río Mayer Formation and green sandstones of Río Belgrano Formation. Sampled level RB-05 is indicated. (For interpretation of the references to color in this figure legend, the reader is referred to the web version of this article.)

grains are cemented by silica, oxides and carbonate. **Sample RT-03** is a poorly sorted coarse-grained litharenite. Grains are dominated by lithics and less monocrystalline quartz, polycrystalline quartz and plagioclase. Subrounded lithic fragments are from volcanic and metamorphic origin. Cement is compound of oxides and carbonates. **Sample RT-10** is a vitric rhyolitic tuff with crystals of quartz and plagioclase in a devitrified matrix.

4.2. Detrital zircon geochronology

The zircon grains were separated from 5 kg samples of a thin greenish sandstone (RB-05), a red fine conglomerate (RT-03), and one tuff layer (RT-10). Heavy mineral fractions were concentrated and separated into 100, 150 and 250 μm size fractions by standard crushing and panning at the Universidad de Buenos Aires. Zircon fractions of roughly 400 grains were handpicked in alcohol under a binocular microscope for geochronology analysis. Zircons of unknowns and standards were handpicked under the microscope and mounted in a 1-inch diameter epoxy puck and slightly ground and polished to expose the surface and keep as much material as possible for laser ablation analyses.

After cathodoluminescence imaging at University of Idaho, the LA-ICP-MS U–Pb analyses were conducted using a New Wave Nd:YAG UV 213-nm laser coupled to a Thermo Finnigan Element 2 single collector, double-focusing, magnetic sector ICP-MS. Operating procedures and parameters were similar to those of Chang et al. (2006). Laser spot size and repetition rate were 30 microns and 10 Hz, respectively. He and Ar carrier gases delivered the sample aerosol to the plasma. Each analysis consists of a short blank analysis followed by 250 sweeps through masses 202, 204, 206, 207, 208, 232, 235, and 238, taking approximately 30 s. Time-independent fractionation was corrected by normalizing U/Pb and Pb/Pb ratios of the unknowns to the zircon standards (Chang et al., 2006). U and Th concentration were monitored by comparing to NIST 610 trace element glass. Two zircon standards were used: Plesovice, with an age of 338 Ma (Sláma et al., 2008) and FC-1, with an age of 1099 Ma (Paces and Miller, 1993). Uranium–lead ages and plots were calculated using Isoplot (Ludwig, 2003). The analyses were corrected by assuming concordance and applying a common Pb correction using the 207 Pb method (Williams, 1998). The analytical data are reported in Table S1 of Supplementary Material, including uncertainties at the 1σ level, and measurement errors. Tera-Wasserburg concordia diagrams for the detrital samples are shown in Supplementary Fig. S1.

4.3. Estimation of maximum depositional ages from detrital zircons

To estimate the maximum depositional ages, we used (1) the youngest graphical peak and (2) the weighted mean of the coherent group of youngest grain ages that overlap at 2σ analytical error. These methods were used successfully in the southern depocenter of the Austral basin in Tierra del Fuego (Fig. 1; Barbeau et al., 2009). An alternative estimate based on the youngest single grain is sometimes valid, but is statistically less valid (Dickinson and Gehrels, 2009). The presence of a well-dated Cretaceous magmatic arc a few kilometers to the west of the studied samples, increases our chances of finding a group of zircons contemporaneous with sedimentation. The age distribution of youngest zircons was initially assessed using the *Tuffzirc* algorithm (Ludwig, 2003) to look for the set of data that formed the tightest cluster of significant ages.

5. Results

5.1. Zircon morphology and U–Pb data

The zircon grains of **sample RB-05** are characterized by the predominance of a population of crystal with prismatic habit and elongation between 3 and 4 (more than 5 is rare); their forms are mainly idiomorphic to subidiomorphic and many grains preserve bipyramidal crystal form (Fig. S2 Online Supplementary Material). The size varies between 100 μm and 250 μm in length. The cathodoluminescence images show crystal grains with oscillatory zoning that suggests a magmatic origin for most of the analyzed zircons (Fig. S2). The spectrum of the 94 obtained ages is between 115 Ma and 1054 Ma (Table S1). The distribution of the ages is characterized by bimodal graphical peaks at ~122 Ma and 182 Ma (Fig. 6A); there are also isolated ages in the Triassic (236 Ma), Permian (255 Ma), Devonian (410, 419 Ma), Silurian (442 Ma), Ordovician (475 Ma), Cambrian (511 Ma), Neoproterozoic (641, 666 Ma), and Mesoproterozoic (1011, 1054 Ma). The youngest graphical peak at ~122 Ma is included in an interval of ages between 115 Ma and 137 Ma (36%) and the peak at ~182 Ma is within the interval 170 to 189 Ma (40%).

The youngest ages from the graphical peak at ~122 Ma were assessed with the *Tuffzirc* algorithm (Ludwig, 2003). The algorithm removed the two youngest grains that were, however, inconsistent with the stratigraphic age. The following 19 zircons formed the youngest significant cluster of overlapping ages. The weighted mean age of the cluster is 122 ± 1 Ma [0.8%] 95% confidence, with a mean square of weighted deviates of 1.2 and a probability = 0.21.

The zircon grains of **sample RT-03** showed some differences with respect to those of sample RB-05, as most of the crystals have prismatic habit (elongation between 2 and 4) but subrounded to rounded forms (Fig. S2). These aspects indicate a higher sediment transport or reworking. The zircons are smaller, ranging between 100 μm and 150 μm in length. The population with idiomorphic prismatic zircons is subordinate. The cathodoluminescence images of the crystals analyzed in RT-03 also showed oscillatory zoning in most of the zircons (Fig. S2). The interval of the 97 detrital zircon ages obtained is between 118 Ma and 2681 Ma (Fig. 6B; Table S1). The pattern of ages has two prominent peaks at ~122 Ma (ages between 118 Ma and 137 Ma; 31%) and ~180 Ma (ages between 170 and 188 Ma; 29%) similar to RB-05 (Fig. 6B). But unlike the previous sample, approximately 30% of the total zircons ages are Paleozoic and Precambrian, with peaks at ~354 Ma (Devonian), 446 Ma (Silurian), and 504 Ma (Cambrian), single ages are in the Neoproterozoic, Mesoproterozoic, and Archean (2681 Ma).

A significant cluster including the youngest 23 grains was found using the Tuffzirc algorithm, coinciding with the consecutive group of youngest grains that overlap at 2σ. The weighted mean of the 23 youngest overlapping ages is 121.5 ± 1.0 Ma [0.75%] 95% confidence, with a mean square of weighted deviates of 1.3 and a probability = 0.17.

The grains separated from the tuff layer (RT-10) are characterized by their prismatic habit with elongation more than 3 and idiomorphic form, many grains preserve bipyramidal crystal faces (Fig. 6C). There were also prismatic zircons with high aspect ratio (elongation more than 5) and inclusions that indicate typically volcanic origin (Fig. S2). 44 zircon grains were chosen for U–Pb dating and the 37 younger ages give a weight age of 112 ± 2 Ma (Fig. 6C) which is interpreted as the depositional age of the tuff.

5.2. Lu–Hf isotope analyses

The Hf isotope composition for 6 zircons separated from RT-10 was analyzed (Table S2). Five Early Cretaceous zircons (~112 Ma) from the sample yielded negative values of initial εHf between −4.5 and −0.8; one Late Jurassic zircon (~157 Ma) has an initial εHf of −5.2. These preliminary εHf negative to neutral values suggest important crustal recycling with some mantle influence.

6. Discussion

6.1. Maximum depositional and tuff ages of the sequence

The stratigraphic age of the Río Belgrano Formation in the studied zone is Barremian based on its abundant ammonoid association of the *Hatchericeras patagonense* zone (Aguirre-Urreta, 2002). The maximum depositional age of RT-03 could be estimated as 115 ± 2 Ma based on the youngest single zircon age. However, a more appropriate assessment, consistent with the stratigraphic age, would be represented by the ~122 Ma graphical peak (Fig. 6A,D). The 122 ± 1 Ma weighted mean age of the youngest significant cluster of overlapping ages is also consistent, and in coincidence with the graphical peak. It should be notice that after an initial assessment with the *Tuffzirc* algorithm, and bearing in mind that they were significantly different from the stratigraphic age, the two youngest grains of 115 ± 2 Ma and 116 ± 2 Ma were consciously not included in the weighted mean age.

The boundaries of the Barremian according to the chronostratigraphic Mesozoic time scale of Cohen et al. (2013) are between ~130 Ma and ~125 Ma. However, the base age of the Aptian is based on the absolute age of the M0r magnetic anomaly, which is still in deep debate, and was defined has 121.2 ± 0.5 Ma (He et al.,

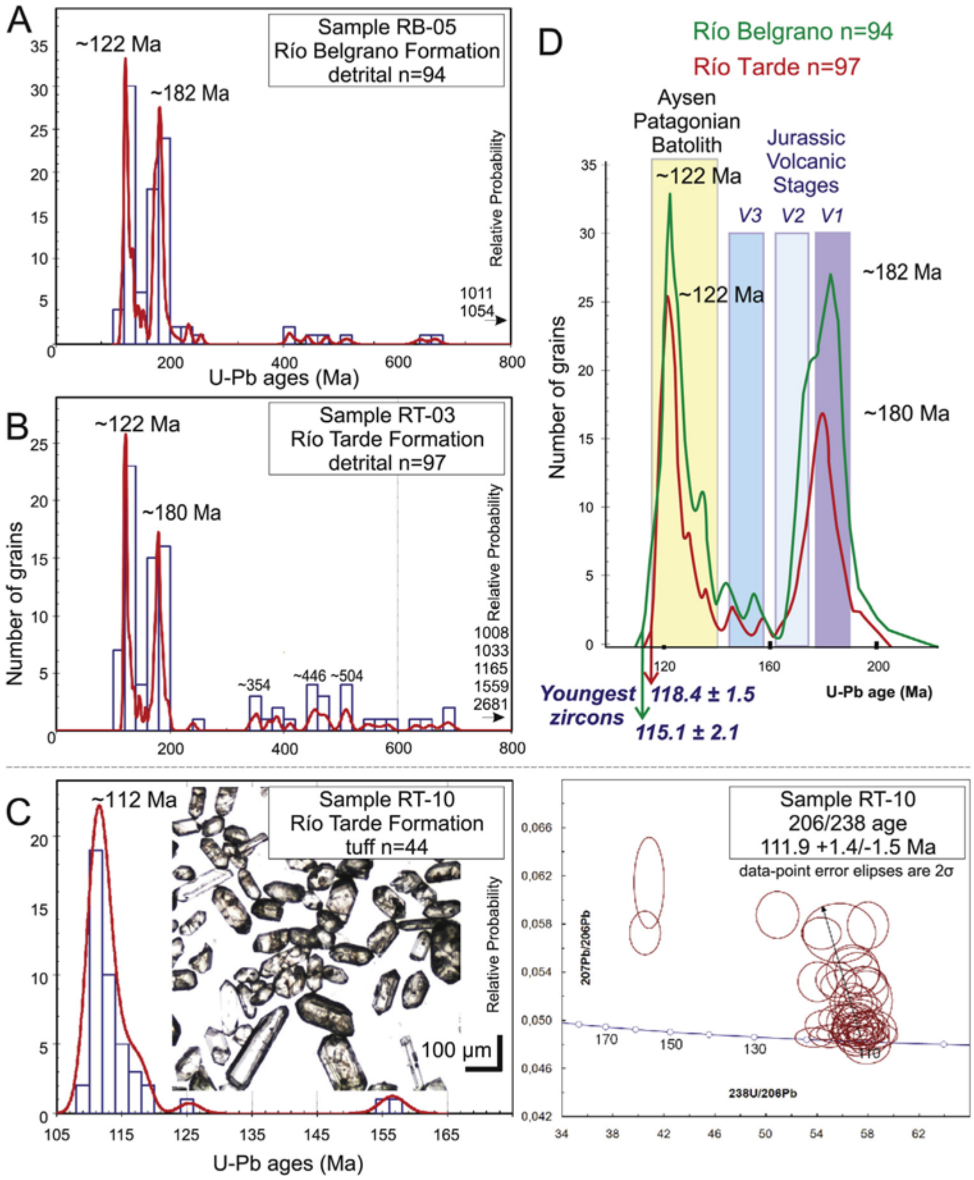

Fig. 6. Frequency histograms with relative probability plots of $^{207}Pb/^{206}Pb$ ages on zircons for (A) detrital sample RB-05, (B) detrital sample RT-03, and (C) tuff sample RT-10 with images of representative zircons and Tera-Wasserburg concordia diagram. (D) Frequency histograms for studied and source units. Data for North Patagonian Batolith in Aysén are from Pankhurst et al. (1999, 2003) and Thomson et al. (2001), and Jurassic Volcanic stages V1-3 are from Pankhurst et al. (2000).

2008). Our U–Pb detrital zircon ages for the basal Río Belgrano Formation indicate a robust measure of the maximum depositional age at ~122 Ma. Therefore our geochronological data and the fossil content are in agreement with the base age of the Aptian calculated by He et al. (2008).

The youngest single zircon of the overlaying red conglomerate of Río Tarde Formation yields an age of 118 ± 2 Ma. However the graphic peak at ~122 Ma is also present (Fig. 6B,D). The weighted mean of the 23 youngest zircons is 121.5 ± 1.0 Ma in agreement with slightly older values for the underlying sample, and constituting a reliable estimation for the maximum depositional age. The ~112 ± 2 Ma tuff indicates the age for the mid section of the upper Río Tarde Formation. Tuffs at the top yielded K–Ar ages of ~99–97 Ma (Ramos and Drake, 1987). The age of this unit can be constrained to the Aptian-Cenomanian, in agreement with previous stratigraphic considerations (Aguirre-Urreta and Ramos, 1981; Arbe, 2002).

6.2. Possible source areas

The whole depositional ranges of the Río Belgrano and Río Tarde formations, and their precise stratigraphic boundaries are beyond the scope of this paper. However, the presence of ~122 Ma peaks of fresh zircons, allows us to examine provenance at in this particular moment in time (Fig. 6D). Three main regions can be distinguished as potential source areas of sediment supply according to the paleogeography of the northern Austral basin (Fig. 1). The western margin is currently represented by the Patagonian Andes, were an active volcanic arc with a climax of activity in the Cretaceous formed the border at that time (Pankhurst et al., 1999, 2000; Suárez and De la Cruz, 2001). The eastern boundary is defined by the Deseado Massif, while the North Patagonian Massif and the Aysén basin are located to the north-northeast.

The ~122 Ma zircons in the Río Belgrano Formation most probably come from volcanic rocks and tuffs produced by contemporaneous activity (Fig. 6D). The roots of this volcanism are identified in the North Patagonian Batholith of Aysén to the west, with Rb–Sr and U–Pb ages of 130–120 Ma (Pankhurst et al., 1999; Thomson et al., 2001). The peak at ~122 Ma in the Río Tarde Formation probably represents reworked detrital zircons, as indicated by the subrounded to rounded forms of the studied crystals (Fig. S2).

The peak at ~182 Ma and 180 Ma coincides with the V1 volcanic stage. Subordinate ages between 173 and 165 Ma comparable with the V2 volcanic stage are also present in both units (Fig. 6D). However, zircon ages of 157–145 Ma (V3) exposed along the Patagonian basement front to the west (Fig. 3) are poorly represented (Fig. 6D). Therefore, a northeastern-eastern source region represented by the Patagonian massifs is interpreted for the Early to Middle Jurassic zircons.

A well represented group of ages in Río Tarde Formation shows Paleozoic, Neoproterozoic, and Mesoproterozoic sources (27%). These old ages together with a petrographic analysis showing a large proportion of metamorphic clasts (Barberón et al., 2014) indicate exposed igneous-metamorphic sources. This type of rock crops out with similar detrital ages in the Eastern Andean Metamorphic Complex located to the west, and in the Deseado Massif to the east.

In summary, the presence of V1 and V2 volcanic zircons, together with Paleozoic and metamorphic detritus is indicative of sources from the North Patagonian and Deseado massifs (Fig. 1), while the ~122 Ma peak probably represents contemporaneous Andean volcanic activity (Fig. 7A).

6.3. *Stratigraphic correlation with contemporary volcanism and magmatism*

Corbella (2006) correlated the volcanic deposits of the Baqueró Group of extra-Andean Patagonia with the Divisadero Group in the Northern Patagonian Andes. The pyroclastic Baqueró Group has been dated between ~118 and 114 Ma (Corbella, 2001; Césari et al., 2011; Pérez Loinaze et al., 2013), while the Divisadero Formation is geochronologically constrained between 118 and 116 Ma (Pankhurst et al., 2003). Considering our ~122 Ma detrital and 112 ± 2 Ma tuff age the tuffaceous upper member of the Río Tarde Formation is regarded as equivalent to the volcanic Divisadero and Baqueró Groups (Figs. 7B and 8). Regionally, this volcanism can be correlated with the tuff-dominated fluvial succession of the Albian Mina del Carmen Formation, part of the widespread Chubut Group of northern Patagonia (Fitzgerald et al., 1990; Paredes et al., 2013). To the south a correlation can be made with the Kachaike Formation (Figs. 2 and 7B; Riccardi and Rolleri, 1980) of late Aptian - early Cenomanian age, based on ammonite fauna and abundant palynological assemblages (Guler and Archangelsky, 2006; Archangelsky and Llorens, 2005).

Our preliminary εHf negative to neutral values (−4.5 to −0.8) suggest important crustal recycling with some mantle influence for the studied volcanism. However, εHf values from the Patagonian Batholith are in the range +2 to +10 by about 130 Ma, and they remain in this range through to the Neogene (Fanning et al., 2009). In contrast, our negative values for the 122 Ma zircons suggest a

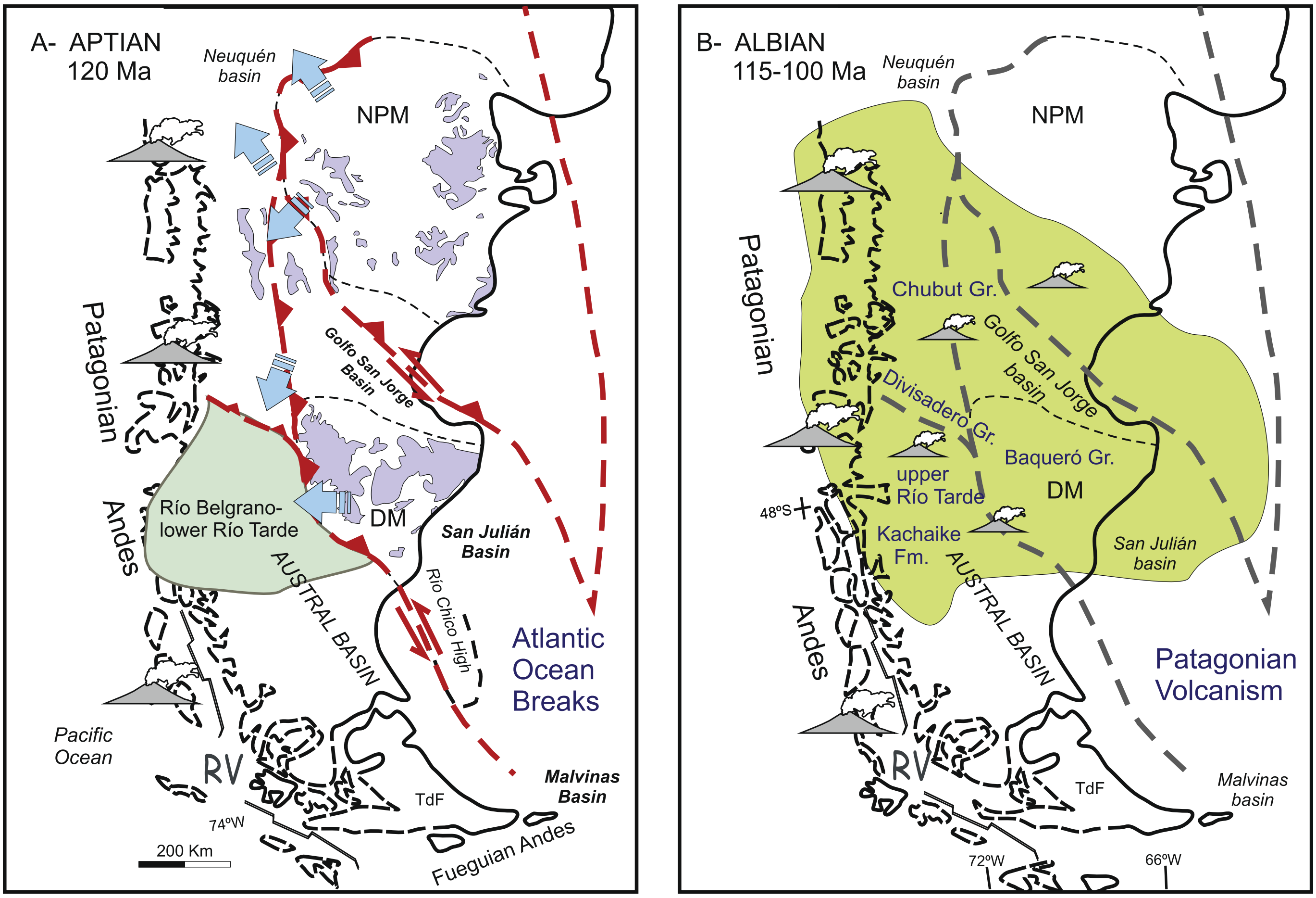

Fig. 7. Proposed conceptual-theoretical geodynamic frame for (A) deposition of Río Belgrano and lower Río Tarde formations during Patagonia uplift, and (B) postorogenic deposition of upper Río Tarde tuffs and correlative units from Patagonia and the Northern Patagonian Andes.

		Lago Pueyrredón	Lago San Martín	San Jorge Basin	North Patagonian Andes	Deseado Massif
Lower Cretaceous	Albian (100.5 Ma – 113 Ma)	upper Río Tarde Formation	Kachaike Fm.	Chubut Gr.: Mina del Carmen Fm.		
	Aptian (113 Ma – 125-121 Ma)			Chubut Gr.: D-129 Fm.	Divisadero Fm.	Baqueró Group
		L. Río Tarde Fm.	Río Mayer Fm.	Cerro Guadal	Coyhaique Group	Bajo Grande Group
	Barrem.-Valangin.	Río Belgrano Fm. Río Mayer Fm.				

Fig. 8. Regional stratigraphic correlation of Early Cretaceous Patagonian volcanism. See text for discussion and references.

stronger crustal influence, probably derived from volcanoes located closer to the craton (Fig. 7B).

6.4. Patagonia and comparison with the Brazilian margin

Our detrital zircon data indicate the exhumation of the Deseado Massif and probably the western rim of the North Patagonian Massif at ~122–118 Ma (Fig. 7A). It coincides with the proposed uplift and deformation of the Deseado and San Julián basins and some sectors of the Deseado Massif (Figueiredo et al., 1996; Soares et al., 2000; Homovc and Constantini, 2001). The contemporaneous uplift of the North Patagonian Andes during the Aptian (Fig. 7A) was identified by Suárez et al. (2010). The uplift of Patagonia can be associated with the latest Barremian-Aptian (Torsvik et al., 2007; Heine et al., 2013) post-breakup deformation and the accelerated opening of the Southern Atlantic Ocean.

A similar response has been registered in SE and NE Brazil, where compressional reactivation of the continental margin started shortly after the formation of an Aptian break-up unconformity (Cobbold et al., 2001; Meisling et al., 2001). The Amazon Basin, which formed in a rift setting during the Paleozoic, went through a phase of strong wrenching between the Early Jurassic and the Cenomanian, but most probably in the mid-Cretaceous (Szatmari, 1983). Right-lateral wrenching acted along the Amazon Basin, while, in the Equatorial Atlantic, Africa was pulling away in a right-lateral sense from South America (Caputo, 1991). The wrenching was responsible for strike-slip faults, reverse faults, and large folds, which uplifted the Precambrian basement (Cobbold et al., 2001; Meisling et al., 2001).

6.5. North–South correlation and implications for the Austral basin

In the light of our detrital and volcanic zircon U–Pb geochronology and stratigraphic correlations, it seems clear that the post-sag depocenter of the Austral basin between 47° and 53°S can be divided into two very distinct segments (Fig. 2): The northern segment extending between Lago Pueyrredón and Lago San Martín presents a 600 m-thick early cycle of Barremian-Albian coarse grained littoral and continental sedimentation (Figs. 4 and 5B). This regressive sedimentation is absent in the segment south of Lago Viedma, were this period corresponds to deep marine facies of the Río Mayer and Zapata formations (Fig. 2). The differences for the Turonian-Paleocene are also striking: while the northern segment presents an important hiatus for that stage (Fig. 5A), the southern segment developed a foreland sequence up to 5000 m thick (Katz, 1963; Wilson, 1991).

The analyses of detrital zircons also show some striking differences and give some clues regarding the paleogeographic boundaries of the Cretaceous Austral basin. The 188–179 Ma ages from the V1 volcanic stage strongly characterizes the northern segment (Fig. 6D). However, this age interval is represented by only 3 grains from a total of 640 analysed in 13 samples of detrital zircons from Punta Barrosa, and younger foreland sequences of the southern depocenter (see Fig. 8 from Romans et al., 2011). The early Barremian-Albian sequences flanked to the east by the Deseado Massif and showing abundant zircons from the V1 and V2 volcanic stages are consistent with sedimentation and subsidence influenced by the exhumation of Patagonia (Fig. 7A). On the other hand, the stacking of Turonian-Paleocene sequences south of 49°S showing western rather than eastern sources (Romans et al., 2011), occurs adjacent to the area influenced by the closure of Rocas Verdes basin and uplift of the Southern Patagonian Andes (Suárez et al. 2010; Ghiglione et al., 2014, in press).

6.6. Neuquén basin

Exhumation of the North Patagonian Massif could also be reflected by a 188–178 Ma detrital zircon population recorded in the Neuquén basin, during deposition of the Aptian-Albian Rayoso Formation (Tunik et al., 2010). This detrital zircon age signal is also present in many other Jurassic and Cretaceous units of the Neuquén basin (Naipauer et al., 2014). Triassic to Middle Jurassic detrital zircons and abundant volcanic lithic fragments recorded in the Neuquén basin during deposition of the Rayoso Formation (Tunik et al., 2010) can be also interpreted as coming from the V1 Jurassic volcanic stage of the North Patagonian Massif (Fig. 7A). Initially, the west-east oriented Huincul High could have acted as a Jurassic-Lower Cretaceous positive element (Chernicoff and Zappettini, 2004) hindering the passage of sediments from the south. However, sedimentological and petrographic analyses, together with paleocurrent orientations suggest that high areas of the North Patagonian Massif were the main source of the fluvial system topping the Late Cretaceous Neuquén Group (Armas et al., 2014).

7. Conclusions

Early Cretaceous continental regressive sequences of the Río Belgrano and Río Tarde formations cover marine facies of the Río Mayer Formation. This radical environmental change seems to represents a major tectonic event related to a new regional geodynamic setting. The Río Belgrano and lower Río Tarde formations present mixed basement sources together with zircons from the V1 and V2 Jurassic volcanic stages in samples robustly dated at ~122 Ma. However, zircons of 157–153 Ma representing the V3 Jurassic volcanic stage along the Patagonian basement thrust front to the west are scarce. South of 50°S zircons of V3 age are present in the basal sequences (Romans et al., 2011) reflecting uplift of the Andes on west-directed thrusts, so that their absence in the northern part of the basin shows that these thrusts were not active there.

The combination of basement sources together with 165–188 Ma zircons assigned to the V1 and V2 Jurassic volcanic stages is characteristic of Central Patagonia, and can be found around the Deseado Massif and along the western rim of the North Patagonian Massif. Our data bolster previous ideas for the Aptian tectonic uplift of Patagonia during the breakout phase of the Southern Atlantic Ocean (Fig. 7A). This stage included ridge-push forces, due to accelerated oceanic opening (Ghiglione et al., 2014), combined with strike-slip faulting and transpressional deformation due to accommodation between ridge sections. It is also noteworthy that the dated coarse grained Aptian-Albian regressive sequences are not present to the south (Fig. 2), restricting this sedimentary event to the sector bounding the Deseado Massif (Fig. 7A).

The tuff sequence of the upper Río Tarde Formation yielded a 112 ± 2 Ma absolute age for its middle section, allowing partial correlation with the Baqueró and Chubut groups from Patagonia, the Divisadero Group of the Northern Patagonian Andes, and south with the Kachaike Formation of the Austral basin (Fig. 7B).

Acknowledgments

This work has been carried out by the financial support of grant projects Agencia PICT-2013-1291 and CONICET PIP 2011-2013 0048 awarded to M.C. Ghiglione. The authors are grateful to Parques Nacionales of Argentina for permitting access to *Perito Moreno* National Park. Special thanks to the park rangers at Lago Belgrano, *Comisión de Fomento de* Hipólito Yrigoyen, and the people of Lago Posadas and Familia Fortuny for allowing accesses to outcrops, kind logistical support and assistance. We want to acknowledge the detailed and insightful reviews from Dr. Robert Pankhurst, Editor Dr. Eduardo Koutsoukos and two anonymous reviewers. This is contribution R-152 of the Instituto de Estudios Andinos Don Pablo Groeber (UBA-CONICET).

References

Aguirre-Urreta, M.B., 1990. Paleogeography and biostratigraphy of the Austral basin in Argentina and Chile: An appeal for sound systematic. Episodes 13, 247–255.

Aguirre-Urreta, M.B., 2002. Invertebrados del Cretácico inferior. In: Haller, M.J. (Ed.), Geología y Recursos Naturales de Santa Cruz. Relatorio XV Congreso Geológico Argentino, pp. 439–459.

Aguirre-Urreta, M.B., Ramos, V.A., 1981. Estratigrafía y Paleontología de la Alta Cuenca del Río Roble, provincia de Santa Cruz. VIII Congreso Geológico Argentino, Actas 3, 101–132.

Arbe, H.A., 1986. El Cretácico de la Cuenca Austral: sus ciclos de Sedimentación. Tesis doctoral (Unpublished). Universidad de Buenos Aires, Facultad de Ciencias Exactas y Naturales, Buenos Aires.

Arbe, H.A., 2002. Análisis estratigráfico del Cretácico de la Cuenca Austral. In: Haller, M.J. (Ed.), Geología y Recursos Naturales de Santa Cruz. XV Congreso Geológico Argentino, El Calafate, Relatorio, pp. 103–128.

Archangelsky, A., Llorens, M., 2005. Palinología de la Formación Kachaike, Cretácico Inferior de la Cuenca Austral, provincia de Santa Cruz 2: Esporas. Ameghiniana 42, 311–328.

Armas, P., Moreno, C., Sánchez, M.L., González, F., 2014. Sedimentary palaeoenvironment, petrography, provenance and diagenetic inference of the Anacleto Formation in the Neuquén Basin, Late Cretaceous, Argentina. Journal of South American Earth Sciences 53, 59–76.

Augustsson, C., Münker, C., Bahlburg, H., Fanning, C.M., 2006. Provenance of late Palaeozoic metasediments of the SW South American Gondwana margin: a combined U–Pb and Hf-isotope study of single detrital zircons. Journal of the Geological Society 163, 983–995.

Barbeau, D.L., Olivero, E.B., Swanson-Hysell, N., Zahid, K.M., Murray, K.E., Gehrels, G., 2009. Detrital-zircon geochronology of the eastern Magallanes foreland basin: Implications for late Eocene kinematics of the northern Scotia Arc and Drake Passage. Earth and Planetary Science Letters 284, 489–503.

Barberón, V., Leal, P.R., Naipauer, M., Ronda, G., Ghiglione, M.C., 2014. Estudio de procedencia de areniscas en el Aptiano-Albiano del río Oro, lago Pueyrredón, provincia de Santa Cruz. Actas del XIX Congreso Geológico Argentino. Córdoba.

Baristeas, N., Anka, Z., di Primio, R., Rodriguez, J.F., Marchal, D., Dominguez, F., 2013. New insights into the tectono-stratigraphic evolution of the Malvinas Basin, offshore of the southernmost Argentinean continental margin. Tectonophysics 604, 280–295.

Bernhardt, A., Jobe, Z.R., Grove, M., Lowe, D.R., 2012. Palaeogeography and diachronous infill of an ancient deep-marine foreland basin, Upper Cretaceous Cerro Toro Formation, Magallanes Basin. Basin Research 24, 269–294. http://dx.doi.org/10.1111/j.1365-2117.2011.00528.x.

Bertrand, H., Féraud, G., Haller, M., Luais, B., Martínez, M., Alric, V., Fornari, M., 1999. The mesozoic silicic large igneous province of Patagonia: Geochronology and origin evidenced by Ar/Ar dating and Sr-Nd isotopes. In: Actas South American Symposium on Isotope Geology, 2, pp. 167–169.

Biddle, K.T., Uliana, M.A., Mitchum, R.M., Fitzgerald, M.G., Wright, R.C., 1986. The stratigraphy and structural evolution of the central and eastern Magallanes Basin, southern South America. In: Allen, A., Homewood, P. (Eds.), Foreland Basins. Blackwell Scientific Publications, London, pp. 41–61. International Association of Sedimentologists Special Publication 8.

Calderón, M., Fildani, A., Hervé, F., Fanning, C.M., Weislogel, A., Cordani, U., 2007. Late Jurassic bimodal magmatism in the northern sea-floor remnant of the Rocas Verdes basin, southern Patagonian Andes. Journal of the Geological Society 164, 1011–1022.

Calderón, M., Fosdick, J.C., Warren, C., Massonne, H.-J., Fanning, C.M., Fadel Cury, L., Schwanethal, J., Fonseca, P.E., Galaz, G., Gaytán, D., Hervé, F., 2012. The low-grade Canal de las Montañas Shear Zone and its role in the tectonic emplacement of the Sarmiento Ophiolitic Complex and Late Cretaceous Patagonian Andes orogeny, Chile. Tectonophysics 524, 165–185.

Caputo, M.V., 1991. Solimões megashear: Intraplate tectonics in north-western Brazil. Geology 19, 246–249.

Césari, S.N., Limarino, C.O., Llorens, M., Passalia, M.G., Loinaze, V.P., Vera, E.I., 2011. High-precision late Aptian Pb/U age for the Punta del Barco Formation (Baqueró Group), Santa Cruz Province, Argentina. Journal of South American Earth Sciences 31, 426–431.

Chang, Z., Vervoort, J.D., McClelland, W.C., Knaack, C., 2006. U-Pb dating of zircon by LA-ICP-MS. Geochemistry Geophysics Geosystems 7, 1–14.

Chernicoff, C.J., Zappettini, E.O., 2004. Geophysical evidence for terrane boundaries in south-central Argentina. Gondwana Research 7, 1105–1116.

Cobbold, P.R., Meisling, K.E., Mount, V.S., 2001. Reactivation of an obliquely rifted margin, Campos and Santos basins, southeastern Brazil. American Association of Petroleum Geologists Bulletin 85, 1925–1944.

Cohen, K.M., Finney, S.C., Gibbard, P.L., Fan, J.X., 2013. The ICS International Chronostratigraphic Chart. Episodes 36, 199–204.

Corbella, H., 2001. Tuffs of the Baqueró Group and the Mid-Cretaceous frame extraandean Patagonia, Argentina, 11 Congreso Latinoamericano de Geología and 3 Congreso Uruguayo de Geología (Montevideo) 190 6pp. (on CD).

Corbella, H., 2006. Nuevas determinaciones de edad absoluta para el Grupo Baqueró, Macizo del Deseado, Patagonia extrandina, 15 Congreso Geológico Argentino (El Calafate) (Cd Rom).

Cúneo, R., Ramezani, J., Scasso, R., Pol, D., Escapa, I., Zavattieri, A.M., Bowring, S.A., 2013. High-precision U–Pb geochronology and a new chronostratigraphy for the Cañadón Asfalto Basin, Chubut, central Patagonia: Implications for terrestrial faunal and floral evolution in Jurassic. Gondwana Research 24, 1267–1275.

Dalziel, I.W., Lawver, L.A., Norton, I.O., Gahagan, L.M., 2013. The Scotia Arc: genesis, evolution, global significance. Annual Review of Earth and Planetary Sciences 41, 767–793.

De La Cruz, R., Suárez, M., Belmar, M., Quiroz, D., Bell, M., 2003. Geología del área Coihaique– Balmaceda, Region Aisen del General Carlos Ibáñez del Campo. Servicio Nacional de Geologıa y Minería, Carta Geologica de Chile, Serie Geología Básica 80, 40 pp. Map scale 1:100,000.

Dickinson, W.R., Gehrels, G.E., 2009. Use of U-Pb ages of detrital zircons to infer maximum depositional ages of strata: A test against a Colorado Plateau database. Earth and Planetary Science Letters 288, 115–125. http://dx.doi.org/10.1016/j.epsl.2009.09.013.

Fanning, C.M., Hervé, F., Pankhurst, R.J., Calderón, M., Yaxley, G.M., Holden, P., 2009. Multi dimensional zircon tracking: a case study using the 150 my evolution of the South Patagonian Batholith. 12 Congreso Geológico Chileno. Actas digitales 5 (S12), 4 p., Santiago.

Féraud, G., Alric, V., Fornari, M., Bertrand, H., Haller, M., 1999. 40Ar/39Ar dating of the Jurassic volcanic province of Patagonia: migrating magmatism related to Gondwana break-up and subduction. Earth and Planetary Science Letters 172, 83–96.

Figueiredo, A.M.F., Pellon de Miranda, A., Ferreira, R.F., Zalan, P.V., 1996. Cuenca de San Julián. In: Ramos, V.A., y Turic, M.A. (Eds.), Geología y Recursos Naturales de la Plataforma Continental Argentina, Relatorio 13° Congreso Geológico Argentino y 3° Congreso de Exploración de Hidrocarburos, pp. 193–212. Buenos Aires.

Fildani, A., Hessler, A.M., 2005. Stratigraphic record across a retroarc basin inversion: Rocas Verdes Magallanes Basin, Patagonian Andes. Geological Society of America Bulletin 117, 1596–1614.

Fitzgerald, M.G., Mitchum Jr., R.M., Uliana, M.A., Biddle, K.T., 1990. Evolution of the San Jorge basin, Argentina. American Association of Petroleum Geologists Bulletin 74, 879–920.

Folk, R.L., Andews, P.B., Lewis, D.W., 1970. Detrital sedimentary rock classification and nomenclature for use in New Zeland. New Zeland Journal Geology and Geophysics 13, 937–968.

Fosdick, J.C., Romans, B.W., Fildani, A., Bernhardt, A., Calderón, M., Graham, S.A., 2011. Kinematic evolution of the Patagonian retroarc fold-and-thrust belt and Magallanes foreland basin, Chile and Argentina, 51°30′S. Geological Society of America Bulletin 123, 1679–1698.

Ghiglione, M.C., Suárez, F., Ambrosio, A., Da Poian, G., Cristallini, E.O., Pizzio, M.F., Reinoso, R.M., 2009. Structure and evolution of the Austral basin fold–thrust belt, southern Patagonian Andes. Revista de la Asociación Geológica Argentina 65, 215–226.

Ghiglione, M.C., Quinteros, J., Yagupsky, D., Bonillo-Martínez, P., Hlebszevtich, J., Ramos, V.A., Vergani, G., Figueroa, D., Quesada, S., Zapata, T., 2010. Structure and tectonic history of the foreland basins of southernmost South America. Journal of South American Earth Sciences 29, 262–277.
Ghiglione, M.C., Likerman, J., Barberón, V., Giambiagi, L., Aguirre-Urreta, M.B., Suárez, F., 2014. Geodynamic context for the deposition of coarse-grained deep-water axial channel systems in the Patagonian Andes. Basin Research 26, 726–745.
Ghiglione, M.C., Cuitiño, J., Barberón, V., Ramos, V., 2015. Growth of the Southern Patagonian Andes (46 -53°S) and its relation with subduction processes. In: Folguera, A. (Ed.), Growth of the Southern Andes. Springer ESS Monograph (in press).
Giacosa, R.E., Márquez, M.M., 2002. El basamento paleozoico de la Cordillera Patagónica. In: Haller, M.J. (Ed.), Geología y Recursos Naturales de Santa Cruz. Relatorio 15° Congreso Geológico Argentino, pp. 45–55.
Giacosa, R., Franchi, M., 2001. Hojas Geológicas 4772-III y 4772-IV Lago Belgrano y Lago Posadas, provincia de Santa Cruz. Servicio Geológico Minero Argentino, Boletín, 256.
Giacosa, R., Zubia, M., Sánchez, M., Allard, J., 2010. Meso-Cenozoic tectonics of the southern Patagonian foreland: Structural evolution and implications for Au-Ag veins in the eastern Deseado Region (Santa Cruz, Argentina). Journal of South American Earth Sciences 30, 134–150.
Guler, M.V., Archangelsky, S., 2006. Albian dinoflagellate cysts from the Kachaike Formation, Austral Basin, southwest Argentina. Revista del Museo Argentino de Ciencias Naturales 8, 179–184.
He, H., Pan, Y., Tauxe, L., Qin, H., Zhu, R., 2008. Toward age determination of the M0r (Barremian–Aptian boundary) of the Early Cretaceous. Physics of the Earth and Planetary Interiors 169, 41–48.
Heine, C., Zoethout, J., Müller, R.D., 2013. Kinematics of the South Atlantic rift. Solid Earth 4, 215–253, 2013.
Hervé, F., Pankhurst, R.J., Fanning, C.M., Calderón, M., Yaxley, G.M., 2007. The South Patagonian batholith: 150 My of granite magmatism on a plate margin. Lithos 97, 373–394.
Hervé, F., Calderón, M., Faúndez, V., 2008. The metamorphic complexes of the Patagonian and Fuegian Andes. Geologica Acta 6, 43–53.
Homovc, J.F., 1980. Estudio estratigráfico de la comarca ubicada en el margen septentrional de la meseta Belgrano, en la zona del Lago Posadas, Dpto. Río Chico, provincia de Santa Cruz. Tesis de licenciatura. Universidad de Buenos Aires, (unpublished), Buenos Aires.
Homovc, J.F., Constantini, L., 2001. Hydrocarbon exploration potential within intraplate shear-related depocenters: Deseado and San Julián basins, southern Argentina. American Association of Petroleum Geologists Bulletin 85, 1795–1816.
Iglesia Llanos, M.P., Lanza, R., Riccardi, A.C., Geuna, S.E., Laurenzi, M.A., Ruffini, R., 2003. Palaeomagnetic study of the El Quemado complex and Marifil formation, Patagonian Jurassic igneous province, Argentina. Geophysical Journal International 154, 599–617.
Katz, H.R., 1963. Revision of Cretaceous stratigraphy in Patagonian Cordillera of Última Esperanza, Magallanes Province, Chile. American Association of Petroleum Geologists Bulletin 47, 506–524.
Kraemer, P.E., Riccardi, A.C., 1997. Estratigrafía de la región comprendida entre los lagos Argentino y Viedma, Provincia de Santa Cruz. Revista de la Asociación Geológica Argentina 52, 333–360.
Ludwig, K.R., 2003. Isoplot 3.0-A geochronological toolkit for Microsoft Excel. Special publication 4. Berkeley Geochronology Center, Berkeley, California, 71 p.
McAtamney, J., Klepeis, K., Mehrtens, C., Thomson, S., Betka, P., Rojas, L., Snyder, S., 2011. Along-strike variability of back-arc basin collapse and the initiation of sedimentation in the Magallanes foreland basin, southernmost Andes. Tectonics 30, TC5001.
Meisling, K., Cobbold, P.R., Mount, V.S., 2001. Segmentation of an obliquely rifted margin, Campos and Santos basins, southern Brazil. American Association of Petroleum Geologists Bulletin 85, 1903–1924.
Naipauer, M., Tunik, M., Marques, J.C., Vera, E.A.R., Vujovich, G.I., Pimentel, M.M., Ramos, V.A., 2014. U–Pb detrital zircon ages of Upper Jurassic continental successions: implications for the provenance and absolute age of the Jurassic–Cretaceous boundary in the Neuquén Basin. Geological Society of London, Special Publications 399, SP399–1.
Paces, J., Miller, J., 1993. Precise U-Pb ages of Duluth complex and related mafic intrusions, northeastern Minnesota; geochronological insights to physical, petrogenetic, paleomagnetic, and tectonomagmatic processes associated with the 1.1 Ga midcontinent rift system. Journal of Geophysical Research 98 (B8), 13997–14013.
Pankhurst, R.J., Rapela, C.W., 1995. Production of Jurassic rhyolite by anatexis in the lower crust of Patagonia. Earth and Planetary Science Letters 134, 23–36.
Pankhurst, R.J., Weaver, S.D., Hervé, F., Larrondo, P., 1999. Mesozoic–Cenozoic evolution of the North Patagonian Batholith in Aysen, southern Chile. Journal of the Geological Society of London 156, 673–694.
Pankhurst, R.J., Riley, T.R., Fanning, C.M., Kelley, S.P., 2000. Episodic silicic volcanism in Patagonia and the Antarctic Peninsula: chronology of magmatism associated with the break-up of Gondwana. Journal of Petrology 41, 605–625.
Pankhurst, R.J., Hervé, F., Fanning, C.M., Suárez, M., 2003. Coeval plutonic and volcanic activity in the Patagonian Andes: the Patagonian Batholith and the Ibáñez and Divisadero formations, Aysén, southern Chile, 10 Congreso Geológico Chileno, Concepción, Chile, CD-ROM.
Paredes, J.M., Plazibat, S., Crovetto, C., Stein, J., Cayo, E., Schiuma, A., 2013. Fault kinematics and depocenter evolution of oil-bearing, continental successions of the Mina del Carmen Formation (Albian) in the Golfo San Jorge basin, Argentina. Journal of South American Earth Sciences 46, 63–79.
Pérez Loinaze, V.S., Vera, E.I., Passalia, M.G., Llorens, M., Friedman, R., Limarino, C.O., Césari, S.N., 2013. High-precision Ue-Pb zircon age from the Anfiteatro de Ticó Formation: Implications for the timing of the early angiosperm diversification in Patagonia. Journal of South American Earth Sciences 48, 97–105.
Ramos, V.A., 1989. Foothills structure in Northern Magallanes Basin, Argentina. American Association of Petroleum Geologists Bulletin 73, 887–903.
Ramos, V.A., Drake, R., 1987. Edad y significado de la Formación Río Tarde (Cretácico), Lago Posadas, Provincia de Santa Cruz. X Congreso Geológico Argentino, Actas I, 143–147, Buenos Aires.
Ramos, V.A., Ghiglione, M.C., 2008. Tectonic evolution of the Patagonian Andes. In: Rabassa, J. (Ed.), Late Cenozoic of Patagonia and Tierra del Fuego. Elsevier, pp. 57–71. Developments in Quaternary Science 11.
Ramos, V.A., Naipauer, M., 2014. Patagonia: where does it come from? Journal of Iberian Geology 40, 367–379.
Riccardi, A.C., Rolleri, E., 1980. Cordillera Patagónica Austral. II Simposio de Geología Regional Argentina, Academia Nacional de Ciencias, Córdoba, pp. 1173–1306.
Romans, B.W., Fildani, A., Hubbard, S.M., Covault, J.A., Fosdick, J.C., Graham, S.A., 2011. Evolution of deepwater stratigraphic architecture, Magallanes Basin, Chile. Marine and Petroleum Geology 28, 612–628.
Sláma, J., Kosler, J., Condon, D.J., Crowley, J.L., Gerdes, A., Hanchar, J.M., Horstwood, M.S.A., Morris, G.A., Nasdala, L., Norberg, N., Schaltegger, U., Schoene, B., Tubrett, M.N., Whitehouse, M.J., 2008. Plesovice zircon – a new natural reference material for U-Pb and Hf isotopic microanalysis. Chemical Geology 249, 1–35.
Soares, F., Miranda, A.P., Figueiredo, A.M.F.D., 2000. Geological and geophysical interpretation of the San Julian Basin—offshore Argentina. Atlantic Rifts and Continental Margins, pp. 193–209.
Suárez, M., De la Cruz, R., 2001. Jurassic to Miocene K–Ar dates from eastern central Patagonian Cordillera plutons, Chile (45–48 S). Geological Magazine 138, 53–66.
Suárez, M., De La Cruz, R., Bell, M., Demant, A., 2010. Cretaceous slab segmentation in southwestern Gondwana. Geological Magazine 147, 193–205.
Szatmari, P., 1983. Amazon rift and Pisco-Juruá fault: their relations to the separation of North America from Gondwana. Geology 2, 300–304.
Thomson, S.N., Hervé, F., Stockhert, B., 2001. The Mesozoic-Cenozoic denudation history of the Patagonian Andes (southern Chile) and its correlation to diferent subduction processes. Tectonics 20, 693–711.
Torsvik, T.H., Rousse, S., Labails, C., Smethurst, M.A., 2007. A new scheme for the opening of the South Atlantic Ocean and the dissection of an Aptian salt basin. Geophysical Journal International 177, 1315–1333.
Tunik, M., Folguera, A., Naipauer, M., Pimentel, M.M., Ramos, V.A., 2010. Early uplift and orogenic deformation in the Neuquén Basin: constraints on the Andean uplift from U–Pb and Hf isotopic data of detrital zircons. Tectonophysics 489, 258–273.
Uliana, M.A., Biddle, K.T., Cerdán, J., 1989. Mesozoic extension and the formation of argentine sedimentary basins. In: Tankard, A.J., Balkwill, H.R. (Eds.), Extensional deformation and stratigraphy of the North Atlantic margins, American Association of Petroleum Geologists Memoire, 46, pp. 599–614.
Varela, A.N., Poiré, D.G., Martin, T., Gerdes, A., Goin, F.J., Gelfo, J.N., Hoffmann, S., 2012. U-Pb zircon constraints on the age of the Cretaceous Mata Amarilla Formation, Southern Patagonia, Argentina: its relationship with the evolution of the Austral Basin. Andean Geology 39, 359–379.
Welkner, D., Godoy, E., Bernhardt, H.J., 2002. Peralkaline rocks in the Late Cretaceous Del Salto Pluton, Eastern Patagonian Andes, Aisén, Chile (47° 35′S). Revista geológica de Chile 29, 3–15.
Williams, I.S., 1998. U-Th-Pb geochronology by ion microprobe. Reviews in Economic Geology 7, 1–35.
Wilson, T.J., 1991. Transition from Back-Arc to Foreland Basin Development in the Southernmost Andes – Stratigraphic Record from the Última-Esperanza-District, Chile. Geological Society of America 103, 98–111.

Appendix A. Supplementary data

Supplementary data related to this article can be found at http://dx.doi.org/10.1016/j.cretres.2015.02.006.